



Magnetic Resonance Imaging of Cerebral Malaria Patients Reveals Distinct Pathogenetic Processes in Different Parts of the Brain

Sanjib Mohanty,^a Laura A. Benjamin,^b Megharay Majhi,^c Premanand Panda,^c Sam Kampondeni,^d Praveen K. Sahu,^a Akshaya Mohanty,^e Kishore C. Mahanta,^f Rajyabardhan Pattnaik,^f Rashmi R. Mohanty,^g Sonia Joshi,^g Anita Mohanty,^f Ian W. Turnbull,^h Arjen M. Dondorp,^{i,j} Terrie E. Taylor,^{k,l}  Samuel C. Wassmer^m

Center for the Study of Complex Malaria in India, Ispat General Hospital, Rourkela, Odisha, India^a; Brain Infections Group, Institute of Infection and Global Health, University of Liverpool, Liverpool, United Kingdom^b; Department of Radiology, Ispat General Hospital, Rourkela, Odisha, India^c; Department of Radiology, Queen Elizabeth Central Hospital, Blantyre, Malawi^d; Infectious Diseases Biology Unit, Institute of Life Sciences, Bhubaneswar, Odisha, India^e; Department of Intensive Care, Ispat General Hospital, Rourkela, Odisha, India^f; Department of Ophthalmology, Ispat General Hospital, Rourkela, Odisha, India^g; North Manchester General Hospital, Manchester, United Kingdom^h; Faculty of Tropical Medicine, Mahidol University, Bangkok, Thailandⁱ; Centre for Tropical Medicine and Global Health, Nuffield Department of Clinical Medicine, Oxford, United Kingdom^j; Department of Osteopathic Medical Specialties, College of Osteopathic Medicine, Michigan State University, East Lansing, Michigan, USA^k; Blantyre Malaria Project, University of Malawi College of Medicine, Blantyre, Malawi^l; Department of Immunology and Infection, London School of Hygiene & Tropical Medicine, London, United Kingdom^m

ABSTRACT The mechanisms underlying the rapidly reversible brain swelling described in patients with cerebral malaria (CM) are unknown. Using a 1.5-Tesla (T) magnetic resonance imaging (MRI) scanner, we undertook an observational study in Rourkela, India, of 11 Indian patients hospitalized with CM and increased brain volume. Among the 11 cases, there were 5 adults and 6 children. All patients had reduced consciousness and various degrees of cortical swelling at baseline. The latter was predominately posterior in distribution. The findings on diffusion-weighted imaging (DWI) and apparent diffusion coefficient (ADC) maps were consistent with vasogenic edema in all cases. Reversibility after 48 to 72 h was observed in >90% of cases. DWI/ADC mismatch suggested the additional presence of cytotoxic edema in the basal nuclei of 5 patients; all of these had perfusion parameters consistent with vascular engorgement and not with ischemic infarcts. Our results suggest that an impairment of the blood-brain barrier is responsible for the brain swelling in CM. In 5 cases, vasogenic edema occurred in conjunction with changes in the basal nuclei consistent with venous congestion, likely to be caused by the sequestration of *Plasmodium falciparum*-infected erythrocytes. While both mechanisms have been individually postulated to play an important role in the development of CM, this is the first demonstration of their concurrent involvement in different parts of the brain. The clinical and radiological characteristics observed in the majority of our patients are consistent with posterior reversible encephalopathy syndrome (PRES), and we show for the first time a high frequency of PRES in the context of CM.

IMPORTANCE The pathophysiology and molecular mechanisms underlying cerebral malaria (CM) are still poorly understood. Recent neuroimaging studies demonstrated that brain swelling is a common feature in CM and a major contributor to death in pediatric patients. Consequently, determining the precise mechanisms responsible for this swelling could open new adjunct therapeutic avenues in CM patients. Using an MRI scanner with a higher resolution than the ones used in previous reports, we

Received 28 April 2017 Accepted 9 May 2017 Published 7 June 2017

Citation Mohanty S, Benjamin LA, Majhi M, Panda P, Kampondeni S, Sahu PK, Mohanty A, Mahanta KC, Pattnaik R, Mohanty RR, Joshi S, Mohanty A, Turnbull IW, Dondorp AM, Taylor TE, Wassmer SC. 2017. Magnetic resonance imaging of cerebral malaria patients reveals distinct pathogenetic processes in different parts of the brain. *mSphere* 2:e00193-17. <https://doi.org/10.1128/mSphere.00193-17>.

Editor Ira J. Blader, University at Buffalo

Copyright © 2017 Mohanty et al. This is an open-access article distributed under the terms of the [Creative Commons Attribution 4.0 International license](https://creativecommons.org/licenses/by/4.0/).

Address correspondence to Samuel C. Wassmer, sam.wassmer@shmt.ac.uk.

identified two distinct origins of brain swelling in both adult and pediatric patients from India, occurring in distinct parts of the brain. Our results support the hypothesis that both endothelial dysfunction and microvascular obstruction by *Plasmodium falciparum*-infected erythrocytes make independent contributions to the pathogenesis of CM, providing opportunities for novel therapeutic interventions.

KEYWORDS MRI, PRES, *Plasmodium falciparum*, vasogenic edema, cerebral malaria

Plasmodium falciparum malaria is a complex disease with a broad spectrum of manifestations. The pathophysiology of cerebral malaria (CM), its most severe form, is still poorly understood. During the past decade, magnetic resonance imaging (MRI) facilities have become increasingly accessible in countries where malaria is endemic, creating new opportunities to investigate the mechanisms underlying the occurrence of CM in living patients (1).

By allowing the comparison of specific parameters between CM patients who survive and those who succumb to the disease, the systematic use of MRI in an extensive study performed in patients from Malawi demonstrated the importance of increased brain volume as a major contributor to death in pediatric CM. The cerebral swelling is transient and quickly reversible with routine treatment in survivors but is associated with progression to herniation and respiratory arrest in fatal cases (2). This general mechanism is consistent with the rapid and complete recovery observed in the majority of surviving cases, and while various hypotheses have been suggested, the cellular pathogenesis underlying the rapidly reversible coma in CM remains unknown (3–5).

In this study, we performed serial brain scans in 11 patients with CM from India who presented with increased brain volume on MRI to investigate the pathophysiology of brain swelling in CM.

RESULTS

Clinical course. During the study period, 27 patients with CM were admitted to Ispat General Hospital (IGH). Three of the patients died shortly after admission and treatment and did not undergo MRI; 24 survived (88.8%). Eleven of these patients had an MRI abnormality at baseline consistent with increased brain volume and were included in our study. These 11 nonfatal CM cases formed the basis of our analysis (Fig. 1). There were five adult and six pediatric patients. The median (range) age was 29 (22 to 40) years for adults and 12 (5 to 15) years for children. There were 4 (80%) adult and 5 (83.3%) pediatric male cases. All patients were comatose (i.e., Glasgow coma score [GCS] of ≤ 9 of 15 or Blantyre coma score [BCS] of ≤ 2 of 5) at baseline. Three of five (60%) adults had a GCS of 15 by 72 h, and all were fully recovered by 1 month, whereas in the pediatric cases, 5/6 (83.3%) had a GCS of 15 by 72 h, and all were fully recovered by 1 month. Overall, rapid recovery was seen in all 11 patients. Key clinical features, complications, and retinal findings are detailed in Table 1. None of the patients had sickle cells. All patients had complete neurological recovery; there were no fatalities.

MRI findings. All 11 cases in our series had generalized swelling (involving >2 lobes); the swelling was marked in 5/11 (45%) patients, moderate in 4/11 (36%), and mild in 2/11 (18%). All 11 had cortical thickening, which was either unilateral (2/11, 18%) or bilateral (9/11, 81.8%). An increased signal on axial T2-weighted and fluid-attenuated inversion recovery (T2/FLAIR) was present in all cases during the first scan, and in 8/11 (72.7%) cases, the distribution was posterior, involving the occipital/parietal and temporal lobes and sparing the frontal lobe (Fig. 2A and B). After 48 to 72 h, complete or nearly complete resolution of cortical thickening and T2/FLAIR signal was seen in all the adult cases and 3/6 (50%) pediatric cases (Fig. 2C and D). Among the latter group, the three remaining patients did not undergo an additional scan but remained clinically well (Table 1).

(i) Vasogenic and cytotoxic edema. There was evidence of vasogenic edema in all 11 patients scanned (Fig. 3 and 4A and B). The severity of vasogenic edema was variable

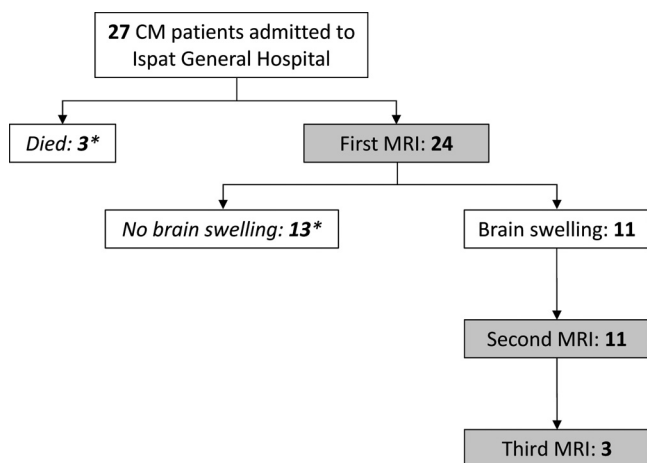


FIG 1 Flowchart of the study. Of the initial 27 patients enrolled in the study, 3 patients died before undergoing MRI and 24 were scanned. Thirteen patients had no brain swelling and were not included in the present analysis. Eleven patients had brain swelling and underwent one ($n = 11$) or two ($n = 3$) additional scans. Patients not included in the study are indicated by an asterisk.

and accounted for the degree of brain swelling described above. In five patients, there were patchy areas of diffusion-weighted imaging/apparent diffusion coefficient (DWI/ADC) mismatch, consistent with ischemia and cytotoxic edema. Cerebral blood volume (CBV), cerebral blood flow (CBF), and mean transit time (MTT) were also captured, and the kinetics of perfusion were analyzed on a regional basis. In these patients, the increased CBV, minimally delayed CBF, and slow MTT were consistent with vascular engorgement (Fig. 4C to E). In all cases, both features reversed rapidly upon treatment (Fig. 4F and G).

(ii) PRES. Because of the posterior predominance of the radiological features and the rapid clinical improvement following antimalarial treatment, we sought to explore in more detail the features of posterior reversible encephalopathy syndrome (PRES) in these cases. All had vasogenic edema, and the imaging abnormalities were mostly posterior, as described above. The changes were predominately cortical in 7/11 (63.7%) patients and infrequently involved the subcortical regions (4/11, 36.3%). Nine of the 11 (82%) had bilateral changes, while two were strictly unilateral. Many of the features discussed above are consistent with PRES. However, the presence of vascular engorgement observed in five patients (cases ID6, ID28, ID60, ID41, and ID46) is not consistent, and thus, the term PRES-like was used. No patients had high blood pressure or were taking drugs associated with PRES prior to their admission (Table 1). Two adult patients had renal impairment.

Malarial retinopathy. Retinal hemorrhages were observed in 5 of the 11 patients (45%). Three patients had hemorrhages on admission, which were reversible within 48 to 72 h in one patient, stayed unchanged in another patient, and worsened in the third. Two patients developed retinal hemorrhages 48 to 72 h postadmission. Hemorrhages were resolved in all patients at follow-up (Table 1). No other features of retinopathy were observed.

DISCUSSION

In a comprehensive MRI analysis of 11 nonfatal pediatric and adult CM cases with increased brain volume, we report observations consistent with vasogenic edema, involving the posterior part of the brain in all cases. Five of these patients had concomitant MRI signatures of vascular congestion in their basal nuclei, reflecting involvement of the deep venous system and its tributaries. All patients presented clinical and radiological evidence of rapid reversibility after antimalarial treatment. Some of the changes we report here are hallmarks of posterior reversible encephalop-

Downloaded from <http://msphere.asm.org/> on May 4, 2018 by guest

TABLE 1 Summary of the clinical, retinal, and MRI findings in 11 Indian patients with nonfatal CM and with PRES or PRES-like features

Patient group, ID ^a	Age	Sex ^b	Key clinical features (no. of seizures; drug history; BP [mm Hg]; creatinine [mg/dl]) ^c	Highest temp (°F)	MRI 1 (10 h)			Clinical features (10 h) ^e			Associated clinical features (48–72 h)			Associated clinical features (1 mo)			Classification				
					Features	Type of edema ^d	GCS	Ret	Comp	Parasitemia (parasites/ μ l)	Features of MRI 2 (48–72 h)	GCS	Ret	Comp	Parasitemia (parasites/ μ l)	Features of MRI 3 (1 mo)		GCS	Ret	Comp	
Adults 6	40	F	2; NA; 120/80; 1.0	99	Marked generalized thickness of cortex in right parieto-occipital region; features of vascular engorgement	Vasogenic edema with some features of ischemia consistent with vascular engorgement	6/15	—	No	291	Nearly complete resolutions of cortical changes	15/15	NP	No	Clear	NP	15/15	NP	No	Clear	PRES-like
17	32	M	2; 0; BP; 120/80; 1.6	98.6	Marked generalized thickening of entire cortical mantle; bilateral effacement of sulci in posterior, temporal, parietal, and occipital lobes	Vasogenic edema ^d	5/15	+	Yes (U)	58,178	Nearly complete resolutions of cortical changes	14/15	+	Yes (U) (H [6–20])	Clear	NP	15/15	—	No	Clear	PRES
22	23	M	0; AM + AP; 110/70; 16.5	99.2	Marked generalized thickness of cortical mantle, right hemisphere involvement greater than left; localized effacement of sulci	Vasogenic edema ^d	9/15	—	Yes (U + AKI)	12,372	Nearly complete resolutions of cortical changes	15/15	NP	Yes (AKI)	Clear	Normal findings	15/15	NP	No	Clear	PRES
28	22	M	2; NA; 110/70; 1.1	100.9	Mild generalized thickening of entire cortical mantle; bilateral focal effacement of sulci in parietal and occipital lobes	Vasogenic edema with some features of ischemia consistent with vascular engorgement affecting BG	5/15	+	Yes (U)	12,654	Complete resolutions of cortical changes	14/15	+	No (H [1–5])	Clear	Normal findings	15/15	—	No	Clear	PRES-like
60	29	M	0; AM; 110/90; 3.2	100	Moderate generalized thickening of entire cortical mantle; right hemisphere involvement greater than left and posterior greater than anterior on each side; generalized sulcal effacement	Vasogenic edema with some features of ischemia consistent with vascular engorgement affecting BG, thalami, and subcortical WM	6/15	—	Yes (U + AKI)	378	Complete resolutions of cortical changes	15/15	NP	Yes (U)	Clear	NP	15/15	NP	No	Clear	PRES-like

(Continued on next page)

TABLE 1 (Continued)

Patient group, ID ^a	Age	Sex ^b	Key clinical features (no. of seizures; drug history; BP)	Highest creatinine temp (°F)	MRI 1 (10 h)			Clinical features (10 h) ^e			Associated clinical features (48–72 h)				Associated clinical features (1 mo)								
					MRI 1 (10 h) Features			Type of edema ^d	GCS	Ret	Comp	Parasitemia (parasites/ μ l)	Features of MRI 2 (48–72 h)	GCS	Ret	Comp	Parasitemia (parasites/ μ l)	Features of MRI 3 (1 mo)	GCS	Ret	Comp	Parasitemia (parasites/ μ l)	Classification
					Features																		
Children 31	12	M	0; AP; 110/80; 0.5	98.6	Moderate	Vasogenic edema	7/15	—	No	21,931	Partial	resolutions of cortical changes	15/15	+	No	Clear	NPC	15/15	—	No	Clear	PRES	
					generalized thickening of entire cortical mantle with sulcal effacement of temporal, parietal, and occipital lobes								(H [1–5])										
32	15	M	0; AP; 90/60; 0.5	100	Mild generalized thickening of cortical mantle, posterior greater than anterior	Vasogenic edema	9/15	—	No	203	Partial	resolutions of cortical changes	15/15	+	No	Clear	NPC	15/15	—	No	Clear	PRES	
														(H [1–5])									
33	5	M	0; AP; 90/70; 1.3	98.8	Moderate	Vasogenic edema	7/15	—	Yes (J)	12,887	No significant improvement		15/15	—	Yes (J + AKI) ^f	Clear	NPC	15/15	NP	No	Clear	PRES	
					generalized thickening of entire cortical mantle with generalized sulcal effacement, more pronounced in posterior temporal parietal, and occipital lobes																		
41	11	M	0; AM; 130/110; 0.7	99	Marked generalized thickening of entire cortical mantle, global widespread sulcal effacement	Vasogenic edema with some features of ischemia consistent with vascular engorgement affecting subcortical WM	5/15	—	Yes (J)	14,750	Nearly complete	resolutions of cortical changes	15/15	—	Data NA	Clear	Normal findings	15/15	NP	No	Clear	PRES-like	
46	21	F	0; AM; 87/60; 0.5	100	Marked generalized cortical thickening of entire cortical mantle, widespread sulcal effacement in posterior temporal parietal, and occipital lobes	Vasogenic edema with some features of ischemia consistent with vascular engorgement affecting subcortical WM and BG (LN)	9/15	+	Yes (SA [1–5])	163	Nearly complete	resolutions of cortical changes	15/15	—	Data NA	Clear	NP	15/15	NP	No	Clear	PRES-like	

(Continued on next page)

TABLE 1 (Continued)

Patient group, ID ^a	Age	Sex ^b	Imm HgJ; creatinine [mg/dl] ^c	Highest temp (°F)	MRI 1 (10 h)			Clinical features (10 h) ^e			Associated clinical features (48–72 h)				Associated clinical features (1 mo)							
					Features	Type of edema ^d	Parasitemia (parasites/ μ l)	GCS	Ret	Comp	Parasitemia (parasites/ μ l)	Features of MRI 2 (48–72 h)	GCS	Ret	Comp	Parasitemia (parasites/ μ l)	Features of MRI 3 (1 mo)	GCS	Ret	Comp	Parasitemia (parasites/ μ l)	
59	5	M	2; 90/60; 0.7	100.4	Moderate cortical thickening of right frontal, temporal, and parietal lobes, mild cortical thickening of left posterior parietal, and occipital lobes	Vasogenic edema	6/15	—	No	219,097	Nearly complete resolutions of cortical changes	14/15	—	No	200	NP	15/15	NP	No	Clear	Clear	PRES-like

^aID, identification number.

^bF, female; M, male.

^cDrug history, treatment prior to admission; NA, not available; AM, antimalarial drug; AP, antipyretic drug; BP, blood pressure on admission (systolic/diastolic); creatinine, laboratory range is 0.8 to 1.4 mg/dl.

^dBG, basal ganglia; WM, white matter; LN, lentiform nucleus.

^eGCS, Glasgow coma score; Ret, retinopathies; +, present; —, absent; H, hemorrhages (number of retinal hemorrhages); Comp, complication; J, jaundice; AKI, acute kidney injury; SA, severe anemia; NP, not performed (not necessary); NPC, not performed (conscious and noncooperative pediatric patients).

^fPerfusion, CBV, CBF, and MTT were not available.

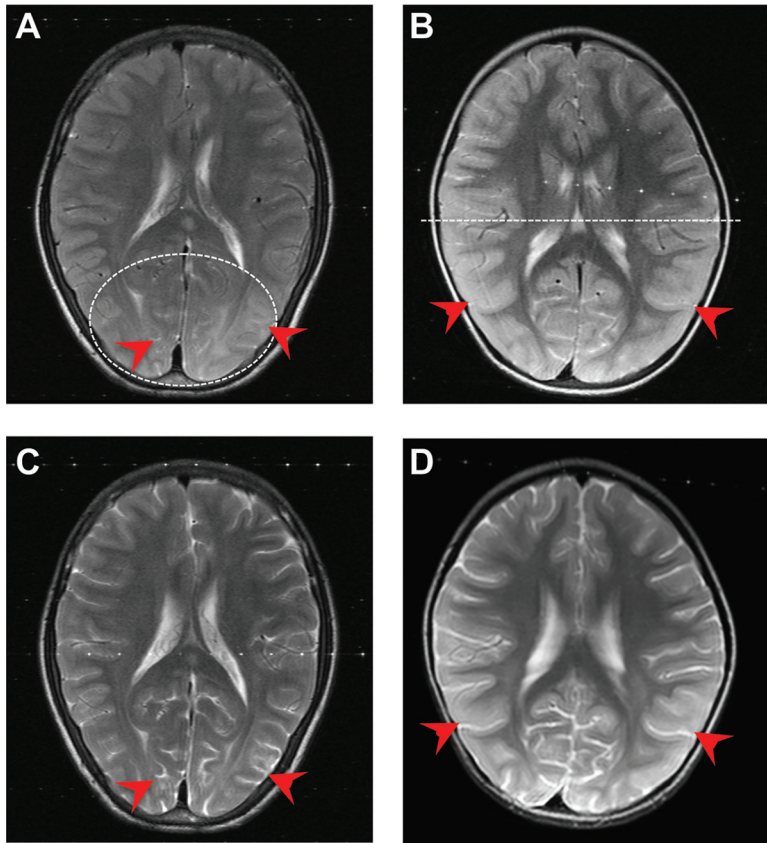


FIG 2 Cases ID32 (left) and ID46 (right). (A, B) Axial T2 images demonstrate a marked cortical thickening of the entire cortical mantle in both patients, with widespread sulcal effacement in the posterior temporal parietal and occipital lobes (red arrows). (C, D) Interval axial T2 images showing nearly complete resolution of the cortical swelling 48 to 72 h postadmission and treatment, with visible sulci (red arrows).

athy syndrome (PRES) and suggest that pathogenetic mechanisms in CM may induce PRES or a PRES-like signature on MRI.

The etiology of brain swelling in CM is unknown but likely to be multifactorial. The microvascular pathology of this neurologic syndrome is unique and mainly caused by the binding of *P. falciparum*-infected erythrocytes (IEs) to vascular endothelium, leading to microvascular obstruction. This phenomenon is called sequestration and is significantly and quantitatively linked to premortem coma in CM patients (6). Adhesive forces causing clumping of parasitized (autoagglutination) and uninfected red cells (rosetting), as well as reduced red cell deformability, are thought to obstruct further microcirculatory flow. In addition, by their adherence to microvascular beds, IEs also induce a broad range of both pathogenetic and protective responses, as well as endothelial activation and signaling. The latter can lead to blood-brain barrier (BBB) leakage, a process previously described in CM patients with various degrees of severity (7–11). Here, we report for the first time that in CM patients with brain swelling, BBB dysfunction occurs in mainly posterior areas of the brain, both in adults and children. The presence and reversibility of retinal hemorrhages in some of our patients did not mirror their cerebral features on MRI, and additional studies are needed to assess the potential correlation between cerebral vascular impairment and retinal hemorrhages in a larger Indian cohort. The local loss of BBB function leads to vasogenic edema, resulting from the plasma leaking into the brain parenchyma. However, evidence for a generalized increase in BBB permeability in CM is still debated (9), and the global distribution of vasogenic edema was only observed in one of our patients. Plugging of microvessels by IE sequestration (12), platelet accretion (13), fibrin thrombi (14), red blood cells with reduced deformability (15), rosetting (16), or a combination of the above (17) can

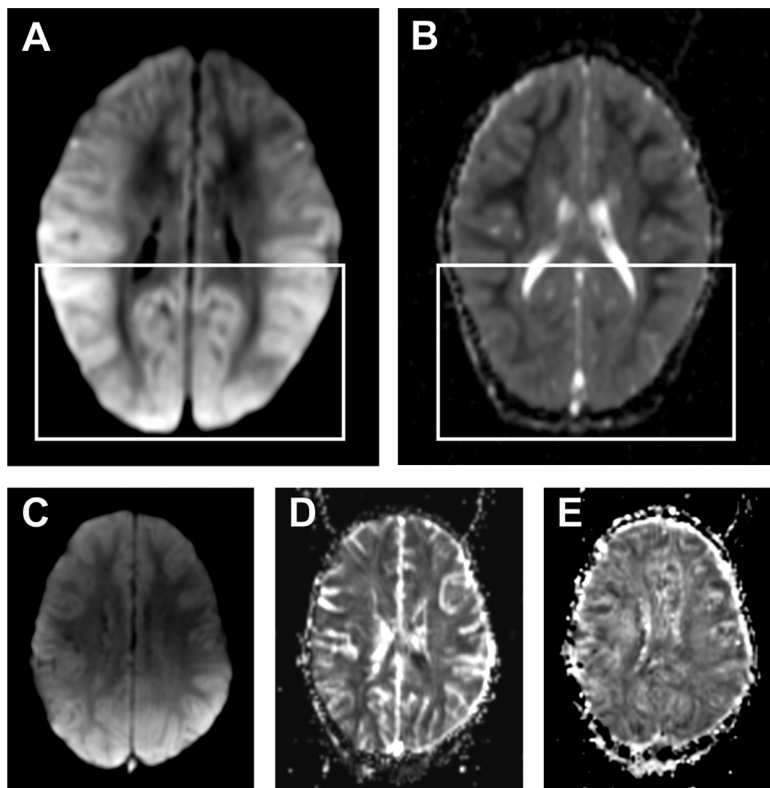


FIG 3 Case ID41. Increased DWI signal in the cortex on admission, with posterior predominance (A) and no mismatch in corresponding ADC image (B), consistent with vasogenic edema (white boxes). Cortical increase of CBF (C) and CBV (D) with minimal reduction of MTT (E) in the same area.

contribute to parenchymal hypoperfusion, as well as to BBB dysfunction from increasing local hypertension. Augmented filtration pressure at the level of the capillary beds could overcome the vascular endothelium and tight intercellular junctions of the BBB, resulting in endothelial dysfunction and surrounding vasogenic edema.

There was evidence of cytotoxic edema (i.e., DWI and ADC mismatch) in 5 of 11 patients, and in this group, the perfusion parameters were more consistent with vascular engorgement than an ischemic event *per se*. Vascular engorgement is an increase in blood volume, which can be caused by arterial vasodilatation or obstruction of the cerebral veins and venous sinuses (18). The intravascular biomass of sequestered IEs may explain the microvascular dilatation and engorgement observed in these patients, thereby contributing to the increase in cerebral volume seen on imaging. This is in line with the positive correlation between microvascular engorgement and coma reported in CM (6). The occurrence of vascular engorgement on MRI was mainly seen in the basal nuclei in our CM cohort. Previous studies showed that these deep and highly vascularized structures of the brain are prone to lacunar strokes, as their penetrating arteries are small and branch directly off a larger, high-pressure, heavily muscled main artery without tapering (19). Such small penetrating arteries may also be particularly vulnerable to IE sequestration, and the resulting decreased perfusion could explain the vascular engorgement of the basal nuclei.

Some of the clinical and radiological characteristics observed in our cohort, namely, the presence of vasogenic edema with posterior presentation and fast reversibility upon treatment, suggest a PRES-like phenomenon. PRES is a clinoradiologic disorder of reversible cortical and/or subcortical brain edema in patients with acute neurological symptoms (seizures, encephalopathy, visual disturbances, and alterations of consciousness) in the setting of a broad range of disorders, including bacterial infection (20). MRI correlates typically include vasogenic edema in the cortex, subcortex, and white

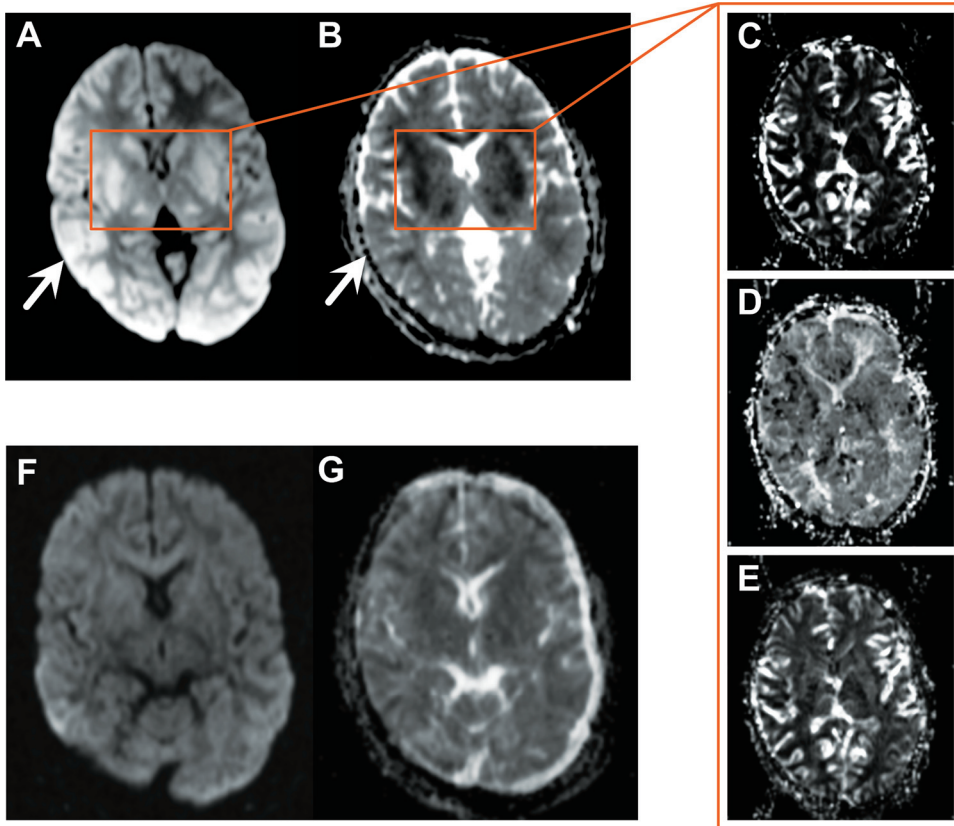


FIG 4 Case ID60. (A to E) Increased DWI signal in the posterior cortex (A, white arrow) with no mismatch in corresponding ADC image (B, white arrow). DWI and ADC mismatch in the basal ganglia (A and B, orange boxes) due to vascular engorgement demonstrated by an increased CBV (C), slightly delayed MTT (D), and nearly normal CBF (E). (F, G) Interval DWI image (F) and corresponding ADC map (G) demonstrating a complete resolution of the lesions 48 to 72 h postadmission and treatment.

matter of the parieto-occipital lobes bilaterally (21); frontal lobe and cerebellar involvement are less frequent (22). A key element of the diagnosis of PRES is the reversibility, which is usually associated with a favorable outcome. However, in its severe form, PRES can be associated with death and disability; posterior fossa edema causing obstructive hydrocephalus is one of the postulated causes of persisting sequelae and death (20, 23).

Although the pathogenesis of PRES remains unclear, impaired cerebral autoregulation caused by the presence of hypertension, drugs (e.g., cyclosporine), or bacterial infections is thought to increase cerebral perfusion, endothelial dysfunction, and breakdown of the BBB, resulting in vasogenic edema (20). These processes are consistent with the disease mechanisms described in CM, and the high frequency of PRES-like presentations we report suggests that an endotheliopathy may be contributing to the pathophysiology of CM in a subset of patients. The predilection for involvement of posterior circulation territories in PRES is suspected to result from the relatively sparse sympathetic innervation of the posterior circulation (24). As sympathetic stimulation is vasoprotective in both hypertensive (25) and endothelial inflammatory (26) causes of PRES, this sympathetic neural network asymmetry would explain why the BBB is more susceptible to dysfunction caused by IE sequestration and subsequent inflammation in the posterior areas during CM. This anterior/posterior difference may have influenced the variability in BBB disruption reported in previous CM histopathology studies, depending on the areas of postmortem brain sampling.

Our understanding of PRES, both in terms of pathogenesis and phenotype, is still evolving (20). Malaria has only been reported as a cause of PRES in one isolated case (27). In the absence of other causes, the underlying etiology of PRES in our series is the

P. falciparum infection. While acute kidney injury is commonly present in patients with PRES or severe malaria, this complication was only observed in two patients and cannot account for the changes observed in the rest of the cohort. Our systematic study of patients in this setting where malaria is endemic underscores for the first time a high frequency of a PRES-like presentation in CM, affecting both adults and children. While cortical involvement with posterior predominance on DWI images was described in some patients from Malawi (2, 28), the lack of ADC maps did not allow the identification of vasogenic edema and, therefore, of PRES. The presence of radiologic signatures of vasogenic edema alone or in conjunction with vascular engorgement in the majority of our patients implicates endothelial dysfunction and sequestration of IEs in the pathogenesis of CM, a theory that was suggested previously (29).

The present study has several limitations. First, it is a small, single-center series of case studies, and further analyses involving higher patient numbers are warranted. Second, we selected 11 of 24 patients with CM based on the presence of abnormalities on MRI, and the mechanisms of coma are likely to be more diverse than described here. In addition, the patient selection was restricted to clinically stable subjects who were able to undergo lengthy MRI scans. Consequently, our results are limited to nonfatal CM, where PRES may correlate with a better outcome. It is plausible that different pathogenetic processes are involved in fatal cases, which could explain the lack of benefit from mannitol, an osmotic diuretic that lowers intracranial pressure by absorbing extracellular fluid into brain capillaries, as an adjunctive therapy in CM (10, 30). Indeed, it is conceivable that ischemic brain injury occurs in fatal cases (31) and develops secondarily after vasogenic edema. Further studies are under way to investigate this hypothesis. Third, although our analysis was focused on patients with changes on baseline MRI, it is possible that the excluded cases may have had subtle changes. Future investigations should consider this cohort to facilitate risk stratification on prognosis. Finally, without angiographic imaging, we were unable to describe the involvement of the vasculature.

In conclusion, our results give new insight into the pathophysiology of reversible brain swelling frequently observed in CM and corroborate the hypotheses suggesting that an impaired BBB and vascular engorgement are contributors to the increased brain volume seen in CM patients. A better understanding of the disease mechanisms and risk stratification on prognosis may provide guidance toward new interventions.

MATERIALS AND METHODS

Study site and patients. The study was carried out at Ispat General Hospital (IGH) in Rourkela, in the state of Odisha, India, from October 2013 to August 2015. All patients satisfied a strict definition of CM according to the modified World Health Organization criteria. Consecutive CM patients with coma (defined as a Glasgow coma score [GCS] of ≤ 9 out of 15 for adults and a Blantyre coma score [BCS] of ≤ 2 for young children) after correction of hypoglycemia (< 2.2 mmol/liter) and infected with *Plasmodium falciparum* (detected by rapid diagnostic test and confirmed by the presence of asexual forms of the parasite in a peripheral blood smear) were eligible for inclusion. Patients who were clinically unstable because of shock (systolic blood pressure of < 80 mm Hg with cool extremities) or signs of respiratory insufficiency (respiratory rate above 40/min, nailbed oxygen saturation $< 90\%$ by pulse oximetry) were excluded because of the increased risk incurred by being transported to the MRI facilities. Other exclusion criteria included the presence of coinfection by other plasmodial species detected by either rapid diagnostic test or peripheral blood smear examination, metallic devices, documented allergies to MRI contrast media, a diagnosis of meningitis or other causes of encephalopathy, and in female patients, pregnancy or lactation. Patients whose relatives did not consent to enrollment or who died within 48 h of admission or regained consciousness before imaging were excluded. Patients with an underlying bacterial infection were also excluded, on the basis of clinical observations and positive blood, urine, or cerebrospinal fluid culture.

Due to the lack of direct association between the presence of retinopathies and CM in low-malaria-transmission settings, retinal changes were documented but not used as a diagnosis parameter in the present cohort. Tonic-clonic seizures were diagnosed based on stereotypical signs and recorded.

Ethics statement. Ethical approval was obtained from The Indian Council of Medical Research (TDR589/2010/ECDII), as well as from the institutional review boards of Ispat General Hospital, New York University School of Medicine (S12-03016), and the London School of Hygiene and Tropical Medicine. Because CM patients are comatose, written informed consent was obtained from the families of all

TABLE 2 Summary of the hematological, biochemical, and other findings in 11 Indian patients with nonfatal CM

Patient group, ID ^a	Hematology ^b					Biochemistry ^c										Other finding		
	Wt (kg)	Height (cm)	Hb (g%)	HCT (%)	PLT ($\times 1,000/\mu\text{l}$)	WBC ($\times 1,000/\mu\text{l}$)	Glucose (mg/dl)	Bilirubin (mg/dl)	GPT/ALT (IU/liter)	Creatinine (mg/dl)	Urea (mg/dl)	Na (mM/liter)	K (mM/liter)	pH	HCO ₃ (mM/liter)	ANA gap (mM/liter)	Blood culture	ECG ^d
Adults																		
6	48	154	10.8	30.3	610	29.1	91	0.2	ND	1	39	142	3.8	ND	ND	ND	ND	ND
17	58	162	10.9	19.3	35	5.3	108	14.2	ND	1.6	149	136	4.7	ND	ND	ND	ND	Normal
22	58	158	14.1	29	28	10.9	100	3.5	107	16.5	117	139	4	7.33	20.2	14	Sterile	ND
28	54	158	10	NA	40	7.4	150	3.3	25	1.1	72	130	4.9	ND	ND	ND	ND	Normal
60	67	155	7.8	24.4	30	15.1	389	6.8	34	3.2	217	131	4.5	ND	ND	ND	ND	ND
Children																		
31	23	142	6.6	NA	62	9.1	138	ND	21	0.5	ND	128	3.2	ND	ND	ND	ND	ND
32	25	142	7.5	NA	102	4.5	ND	ND	24	0.5	ND	135	3.4	ND	ND	ND	ND	ND
33	13	98	10.6	NA	NA	9.8	99	4.5	109	3.3	149	141	3.5	ND	ND	ND	ND	ND
41	22	120	13.6	33.9	44	12.5	210	3.6	90	0.7	76	133	3.6	7.4	27.4	ND	Sterile	Normal
46	12	40	3.2	8.6	25	27.2	ND	2	29	0.5	64	131	5.2	ND	ND	ND	ND	ND
59	12	80	6.3	19.6	26	25.4	10	ND	ND	0.7	47	134	4.8	ND	ND	ND	Sterile	ND

^aID, identification number.

^bHb, hemoglobin; HCT, hematocrit; PLT, platelets; WBC, total white blood cells; NA, not available.

^cGPT/ALT, serum glutamic pyruvic transaminase/alanine transaminase; Na, sodium; K, potassium; HCO₃, serum bicarbonate; ANA gap, anion gap; ND, not done as not requested by the physician in charge.

^dECG, electrocardiogram.

patients (five adults and six children) before enrollment in the study. Following our Institutional Review Board (IRB)-approved clinical protocol, a nurse carefully described the study to the potential participants' families in Oriya, the local language in the state of Odisha. The IRB-approved consent form was then read in its entirety to the families before written consent was sought through signature or inked fingerprint. The nurse in charge of the enrollment and an impartial witness cosigned the form. Patients whose families declined the enrollment were not included in the study. Patient consent has been archived with the authors and is available upon request.

Study procedures. On admission, a full medical history and physical examination were conducted and recorded on a standardized clinical record form. Rapid diagnostic tests for the detection of *Plasmodium falciparum* histidine-rich protein II were used for all patients (SD Bioline; Standard Diagnostics, India). Blood samples were collected for complete blood count, parasite count, hemoglobin, hematocrit, glucose, and biochemistry. Other investigations, including ECG and blood culture, were performed when clinically indicated (Table 2). Blood gases were monitored frequently in patients receiving ventilatory support until they recovered.

Retinal examination. To compare potential differences in pathogenetic processes between retinal and cerebral vasculatures in our cohort of CM cases (32), all patients underwent retinal examination by direct and indirect ophthalmoscopy within 6 h of admission, and the severity of the findings was graded by two ophthalmologists (R. R. Mohanty and S. Joshi) according to published classification criteria (33).

MR imaging. Imaging of the brain was performed using a 1.5-Tesla (T) Siemens Symphony MRI scanner (Siemens AG, Erlangen, Germany). Scanning was carried out initially within 10 h of admission and then again between 48 and 72 h after admission. When MRI abnormalities were identified on the second interval scan, a third scan was performed at approximately 1 month. The MRI sequences included sagittal T1-weighted images, axial T2-weighted and fluid-attenuated inversion recovery (T2/FLAIR) turbo spin echo, susceptibility-weighted imaging (SWI), axial trace diffusion-weighted imaging (DWI) (b values, indicative of the degree of diffusion weighting applied, of 0, 500, and 1,000 s/mm²), and axial T1 spin echo (T1-SE) after contrast (529 mg/ml gadobenate dimeglumine [Multihance]; Bracco Diagnostics). Contrast injection was performed and monitored by automated injector (MedRad Spectris Solaris EP; Bayer). The pulse sequences included T2, FLAIR, T1, and gradient echo. Apparent diffusion coefficient (ADC) maps were generated and used to confirm restricted diffusion (34). Perfusion parameters, such as cerebral blood volume (CBV), cerebral blood flow (CBF), and mean transit time (MTT), were calculated using previously described techniques (35). From these sequences, we were able to locate and characterize lesions in the brain, describe their physiological features, and identify temporal changes. The degree of generalized brain swelling was semiquantified as mild (just discernible), moderate (clearly evident without mass effect), or marked (extensive with mass effect). Vasogenic edema was defined radiologically as an increased DWI signal with markedly increased diffusion coefficients compared with those of normal white matter (36), whereas cytotoxic edema was defined as DWI hyperintensity associated with decreased diffusion coefficients compared with those of white matter (DWI/ADC mismatch) (37).

MRI interpretation. Each MRI was interpreted by two radiologists on-site (M. Majhi and P. Panda) and one experienced radiologist off-site (S. Kampondeni) using NeuroIndia, a searchable database based on a systematic scoring system of brain MRI interpretation derived from NeuroInterp (38). The MR studies and data derived from CBV, CBF, and MTT were analyzed blindly by an independent neuroradiologist off-site (I. W. Turnbull). Discrepant cases were settled by consensus.

Clinical care. All patients were treated with intravenous artesunate (2.4 mg/kg of body weight). The first dose was given immediately after diagnosis and the second and third at 12-h intervals, for a minimum of 3 doses. Subsequent doses were administered daily. Once the patients were conscious and able to take medication orally, the treatment was switched to an artemisinin-based combination therapy: oral artesunate (4 mg/kg of body weight) once daily for 3 days together with a single dose of oral sulfadoxine-pyrimethamine (25 and 1.25 mg/kg of body weight) on the first day of oral therapy. A single gametocytocidal dose of primaquine (0.75 mg/kg of body weight) was given on the second day of oral therapy. These treatments were in accordance with the national drug policy of the Government of India. Disability at discharge or new/progression of symptoms by 1 month were determined and described on the basis of the Glasgow or Blantyre coma score, retinal changes, and cranial nerve and motor system function. When possible, a third MRI scan was performed for patients who had magnetic resonance abnormalities on the second scan.

ACKNOWLEDGMENTS

We thank Saroj Mishra (deceased) and Frederik Barkhof for their invaluable help during the setup of the project, the Director in Charge and the clinical staff of Ispat General Hospital in Rourkela for their support and dedication, and the Director of the Institute of Life Sciences in Bhubaneswar for allowing us to use its Infectious Disease Biology Unit.

This work was supported by the National Institute of Allergy and Infectious Diseases of the National Institutes of Health under award numbers U19AI089676, U19AI089676-01S1 (to S.C.W.), and U19AI089683 (to T.E.T.). L.A.B. is supported by the National Institute for Health Research of Great Britain.

The content is solely the responsibility of the authors and does not necessarily

represent the official views of the National Institutes of Health. The funders had no role in the study design, data collection and interpretation, or the decision to submit the work for publication. None of the authors have any conflicts of interest.

REFERENCES

- Mohanty S, Taylor TE, Kampondeni S, Potchen MJ, Panda P, Majhi M, Mishra SK, Wassmer SC. 2014. Magnetic resonance imaging during life: the key to unlock cerebral malaria pathogenesis? *Malar J* 13:276. <https://doi.org/10.1186/1475-2875-13-276>.
- Seydel KB, Kampondeni SD, Valim C, Potchen MJ, Milner DA, Muwalo FW, Birbeck GL, Bradley WG, Fox LL, Glover SJ, Hammond CA, Heyderman RS, Chilingulo CA, Molyneux ME, Taylor TE. 2015. Brain swelling and death in children with cerebral malaria. *N Engl J Med* 372:1126–1137. <https://doi.org/10.1056/NEJMoa1400116>.
- Eisenhut M. 2015. The evidence for a role of vasospasm in the pathogenesis of cerebral malaria. *Malar J* 14:405. <https://doi.org/10.1186/s12936-015-0928-4>.
- Maude RJ, Beare NA. 2009. Fluorescein angiography findings strengthen the theoretical basis for trialling neuroprotective agents in cerebral malaria. *Trends Parasitol* 25:350–351. <https://doi.org/10.1016/j.pt.2009.05.008>.
- White NJ, Turner GD, Day NP, Dondorp AM. 2013. Lethal malaria: Marchiafava and Bignami were right. *J Infect Dis* 208:192–198. <https://doi.org/10.1093/infdis/jit116>.
- Ponsford MJ, Medana IM, Prapansilp P, Hien TT, Lee SJ, Dondorp AM, Esiri MM, Day NP, White NJ, Turner GD. 2012. Sequestration and microvascular congestion are associated with coma in human cerebral malaria. *J Infect Dis* 205:663–671. <https://doi.org/10.1093/infdis/jir812>.
- Brown H, Hien TT, Day N, Mai NT, Chuong LV, Chau TT, Loc PP, Phu NH, Bethell D, Farrar J, Gatter K, White N, Turner G. 1999. Evidence of blood-brain barrier dysfunction in human cerebral malaria. *Neuropathol Appl Neurobiol* 25:331–340. <https://doi.org/10.1046/j.1365-2990.1999.00188.x>.
- Brown HC, Chau TT, Mai NT, Day NP, Sinh DX, White NJ, Hien TT, Farrar J, Turner GD. 2000. Blood-brain barrier function in cerebral malaria and CNS infections in Vietnam. *Neurology* 55:104–111. <https://doi.org/10.1212/WNL.55.1.104>.
- Medana IM, Day NP, Sachanonta N, Mai NT, Dondorp AM, Pongponratn E, Hien TT, White NJ, Turner GD. 2011. Coma in fatal adult human malaria is not caused by cerebral oedema. *Malar J* 10:267. <https://doi.org/10.1186/1475-2875-10-267>.
- Mohanty S, Mishra SK, Patnaik R, Dutt AK, Pradhan S, Das B, Patnaik J, Mohanty AK, Lee SJ, Dondorp AM. 2011. Brain swelling and mannitol therapy in adult cerebral malaria: a randomized trial. *Clin Infect Dis* 53:349–355. <https://doi.org/10.1093/cid/cir405>.
- Patnaik JK, Das BS, Mishra SK, Mohanty S, Satpathy SK, Mohanty D. 1994. Vascular clogging, mononuclear cell margination, and enhanced vascular permeability in the pathogenesis of human cerebral malaria. *Am J Trop Med Hyg* 51:642–647. <https://doi.org/10.4269/ajtmh.1994.51.642>.
- MacPherson GG, Warrell MJ, White NJ, Looareesuwan S, Warrell DA. 1985. Human cerebral malaria. A quantitative ultrastructural analysis of parasitized erythrocyte sequestration. *Am J Pathol* 119:385–401.
- Grau GE, Mackenzie CD, Carr RA, Redard M, Pizzolato G, Allasia C, Cataldo C, Taylor TE, Molyneux ME. 2003. Platelet accumulation in brain microvessels in fatal pediatric cerebral malaria. *J Infect Dis* 187:461–466. <https://doi.org/10.1086/367960>.
- Moxon CA, Wassmer SC, Milner DA, Jr, Chisala NV, Taylor TE, Seydel KB, Molyneux ME, Faragher B, Esmon CT, Downey C, Toh CH, Craig AG, Heyderman RS. 2013. Loss of endothelial protein C receptors links coagulation and inflammation to parasite sequestration in cerebral malaria in African children. *Blood* 122:842–851. <https://doi.org/10.1182/blood-2013-03-490219>.
- Ishioka H, Ghose A, Charunwatthana P, Maude R, Plewes K, Kingston H, Intharabut B, Woodrow C, Chotivanich K, Sayeed AA, Hasan MU, Day NP, Faiz A, White NJ, Hossain A, Dondorp AM. 2016. Sequestration and red cell deformability as determinants of hyperlactatemia in *Falciparum* malaria. *J Infect Dis* 213:788–793. <https://doi.org/10.1093/infdis/jiv502>.
- Rowe JA, Moulds JM, Newbold CI, Miller LH. 1997. *P. falciparum* rosetting mediated by a parasite-variant erythrocyte membrane protein and complement-receptor 1. *Nature* 388:292–295. <https://doi.org/10.1038/40888>.
- Wassmer SC, Combes V, Grau GER. 2011. Platelets and microparticles in cerebral malaria: the unusual suspects. *Drug Discov Today Dis Mech* 8:e15–e23. <https://doi.org/10.1016/j.ddmec.2011.11.004>.
- Rowland LP, Pedley TA. 2010. Merritt's neurology. Lippincott Williams & Wilkins, Philadelphia, PA.
- Caplan LR. 2015. Lacunar infarction and small vessel disease: pathology and pathophysiology. *J Stroke* 17:2–6. <https://doi.org/10.5853/jos.2015.17.1.2>.
- Fugate JE, Rabinstein AA. 2015. Posterior reversible encephalopathy syndrome: clinical and radiological manifestations, pathophysiology, and outstanding questions. *Lancet Neurol* 14:914–925. [https://doi.org/10.1016/S1474-4422\(15\)00111-8](https://doi.org/10.1016/S1474-4422(15)00111-8).
- Hinchey J, Chaves C, Appignani B, Breen J, Pao L, Wang A, Pessin MS, Lamy C, Mas JL, Caplan LR. 1996. A reversible posterior leukoencephalopathy syndrome. *N Engl J Med* 334:494–500. <https://doi.org/10.1056/NEJM199602223340803>.
- Liman TG, Bohner G, Heuschmann PU, Endres M, Siebert E. 2012. The clinical and radiological spectrum of posterior reversible encephalopathy syndrome: the retrospective Berlin PRES study. *J Neurol* 259:155–164. <https://doi.org/10.1007/s00415-011-6152-4>.
- Bartynski WS, Boardman JF, Zeigler ZR, Shadduck RK, Lister J. 2006. Posterior reversible encephalopathy syndrome in infection, sepsis, and shock. *AJNR Am J Neuroradiol* 27:2179–2190.
- Edvinsson L, Owman C, Sjöberg NO. 1976. Autonomic nerves, mast cells, and amine receptors in human brain vessels. A histochemical and pharmacological study. *Brain Res* 115:377–393. [https://doi.org/10.1016/0006-8993\(76\)90356-5](https://doi.org/10.1016/0006-8993(76)90356-5).
- Chen TY, Lee HJ, Wu TC, Tsui YK. 2009. MR imaging findings of medulla oblongata involvement in posterior reversible encephalopathy syndrome secondary to hypertension. *AJNR Am J Neuroradiol* 30:755–757. <https://doi.org/10.3174/ajnr.A1337>.
- Marra A, Vargas M, Striano P, Del Guercio L, Buonanno P, Servillo G. 2014. Posterior reversible encephalopathy syndrome: the endothelial hypotheses. *Med Hypotheses* 82:619–622. <https://doi.org/10.1016/j.mehy.2014.02.022>.
- Lacout A, Guidoux C, Carlier RY. 2010. Posterior reversible encephalopathy syndrome in neuro-malaria. *Indian J Radiol Imaging* 20:198–201. <https://doi.org/10.4103/0971-3026.69357>.
- Potchen MJ, Kampondeni SD, Seydel KB, Birbeck GL, Hammond CA, Bradley WG, DeMarco JK, Glover SJ, Ugorji JO, Latourette MT, Siebert JE, Molyneux ME, Taylor TE. 2012. Acute brain MRI findings in 120 Malawian children with cerebral malaria: new insights into an ancient disease. *AJNR Am J Neuroradiol* 33:1740–1746. <https://doi.org/10.3174/ajnr.A3035>.
- Hanson J, Lee SJ, Hossain MA, Anstey NM, Charunwatthana P, Maude RJ, Kingston HW, Mishra SK, Mohanty S, Plewes K, Piera K, Hassan MU, Ghose A, Faiz MA, White NJ, Day NP, Dondorp AM. 2015. Microvascular obstruction and endothelial activation are independently associated with the clinical manifestations of severe *falciparum* malaria in adults: an observational study. *BMC Med* 13:122. <https://doi.org/10.1186/s12916-015-0365-9>.
- Namutangula B, Ndeezi G, Byarugaba JS, Tumwine JK. 2007. Mannitol as adjunct therapy for childhood cerebral malaria in Uganda: a randomized clinical trial. *Malar J* 6:138. <https://doi.org/10.1186/1475-2875-6-138>.
- Penet MF, Viola A, Confort-Gouny S, Le Fur Y, Duhamel G, Kober F, Ibarrola D, Izquierdo M, Coltel N, Gharib B, Grau GE, Cozzone PJ. 2005. Imaging experimental cerebral malaria in vivo: significant role of ischemic brain edema. *J Neurosci* 25:7352–7358. <https://doi.org/10.1523/JNEUROSCI.1002-05.2005>.
- Greiner J, Dorovini-Zis K, Taylor TE, Molyneux ME, Beare NA, Kamiza S, White VA. 2015. Correlation of hemorrhage, axonal damage, and blood-tissue barrier disruption in brain and retina of Malawian children with fatal cerebral malaria. *Front Cell Infect Microbiol* 5:18. <https://doi.org/10.3389/fcimb.2015.00018>.
- Harding SP, Lewallen S, Beare NA, Smith A, Taylor TE, Molyneux ME. 2006. Classifying and grading retinal signs in severe malaria. *Trop Doct* 36(Suppl 1):1–13. <https://doi.org/10.1258/004947506776315781>.
- Le Bihan D, Breton E, Lallemand D, Grenier P, Cabanis E, Laval-Jeantet M.

1986. MR imaging of intravoxel incoherent motions: application to diffusion and perfusion in neurologic disorders. *Radiology* 161:401–407. <https://doi.org/10.1148/radiology.161.2.3763909>.
35. Huisman TA, Sorensen AG. 2004. Perfusion-weighted magnetic resonance imaging of the brain: techniques and application in children. *Eur Radiol* 14:59–72. <https://doi.org/10.1007/s00330-003-1972-y>.
36. Sevick RJ, Kanda F, Mintorovitch J, Arieff AI, Kucharczyk J, Tsuruda JS, Norman D, Moseley ME. 1992. Cytotoxic brain edema: assessment with diffusion-weighted MR imaging. *Radiology* 185:687–690. <https://doi.org/10.1148/radiology.185.3.1438745>.
37. Ho ML, Rojas R, Eisenberg RL. 2012. Cerebral edema. *AJR Am J Roentgenol* 199:W258–W273. <https://doi.org/10.2214/AJR.11.8081>.
38. Potchen MJ, Kampondeni SD, Ibrahim K, Bonner J, Seydel KB, Taylor TE, Birbeck GL. 2013. NeuroInterp: a method for facilitating neuroimaging research on cerebral malaria. *Neurology* 81:585–588. <https://doi.org/10.1212/WNL.0b013e31829e6ed5>.